IEEE Access
Multidisciplinary | Rapid Review | Open Access Journal

Received 23 August 2022, accepted 3 September 2022, date of publication 8 September 2022, date of current version 16 September 2022.

Digital Object Identifier 10.1109/ACCESS.2022.3205343

RESEARCH ARTICLE

A DOA Estimation Method for Sparse Array Based on DFT Spectrum of Received Signals

LIYE ZHANG, WEIJIA CUI, BIN BA, CHUNXIAO JIAN, AND HAO LI
National Digital Switching System Engineering and Technological Research Center, Zhengzhou, Henan 450001, China
Corresponding author: Liye Zhang (lyzh940307@163.com)

This work was supported in part by the National Natural Science Foundation of China under Grant 62171468.

ABSTRACT In the direction of arrival (DOA) estimation of sparse array received signals, the estimation accuracy of the grid search method in compressed sensing is improved with the increase of over-complete redundant dictionary elements. However, the increase of over-complete redundant dictionary elements will lead to a significant increase in the computational complexity of this method. In order to reduce the computational complexity caused by over-complete redundant dictionary division, based on the equivalent received signal of large aperture continuous difference co-array generated by sparse array, a DOA estimation method using discrete Fourier transform (DFT) spectrum of signal for initial estimation is proposed in this paper. After obtaining the DFT spectrum of the equivalent signal, based on the correspondence between the DFT spectrum and the actual angle value, this paper proposes a new strategy for dividing the over-complete redundant dictionary. In the process of fine angle search, this paper applies Taylor expansion to orthogonal matching pursuit (OMP) algorithm to obtain higher estimation accuracy. Numerical simulation results demonstrate the advantages of the proposed estimation method over the other methods.

INDEX TERMS Array signal processing, sparse array, DOA estimation, difference co-array.

I. INTRODUCTION

As an important branch of array signal processing, direction of arrival (DOA) estimation is widely used in wireless communication, radar, sonar, unmanned vehicles [1], [2], [3], [4] and other fields. Experts and scholars from various countries have studied a large number of high-resolution estimation algorithms for uniform linear array (ULA), such as multiple signal classification (MUSIC) algorithm [5], estimating signal parameter via rotational invariance techniques (ESPRIT) [6] and their improved algorithms [7], [8], [9]. However, ULA consists of several sensors, the spacing of which does not exceed half wavelength of impinging signal, and there is a large mutual coupling interference between them [10], [11]. In addition, the number of sources estimated by ULA cannot exceed the total number of sensors. If a large number of sources are estimated, it can only be achieved by increasing the number of array sensors, which obviously brings an increase in the cost of array design.

The associate editor coordinating the review of this manuscript and approving it for publication was Manuel Rosa-Zurera.

The sensor spacing of sparse array is not limited by the half-wavelength of the received signal, and compared with ULA, it can provide a larger array aperture in the case of fewer array sensors, thus achieving higher DOA estimation accuracy. At the same time, the co-array obtained by difference of sparse array has more virtual sensors than the actual number of physical sensors, which can provide greater degrees of freedom and increase the number of estimable sources. In addition, under the same array aperture, the number of sensors of sparse array is obviously less than that of ULA, which greatly reduces the cost of array design. Therefore, sparse array design and DOA estimation methods based on sparse array have been widely concerned by experts and scholars at home and abroad. A large number of sparse array structures have been proposed, such as minimum redundant array (MRA) [12], nested array (NA) [13], coprime array (CA) [14] and various improved array structures [15], [16], [17], [18]. At the same time, a series of algorithms to solve the problem of sparse array DOA estimation, such as subspace algorithms based on spatial smoothing (SS), like SS-ESPRIT algorithm [19], algorithms based on DFT method [20], [21]

and algorithms based on compressed sensing method [22], have been proposed and improved successively, which form the theoretical basis of sparse array DOA estimation.

In [19], an equivalent single snapshot received data of a difference co-array is constructed by using the covariance matrix of the received signal, and the full rank semidefinite covariance matrix is constructed by using the spatial smoothing method for the received data. The subspace class algorithm can be used to estimate the DOA of the sparse array. However, spatial smoothing reduces the degree of freedom (DOF) of the sparse array by nearly half, which affects the maximum number of estimable sources. The conventional DFT estimation algorithm proposed in [20] was initially used to solve the problem of DOA estimation of single snapshot received data from large-scale ULAs. Because sparse arrays can obtain co-arrays whose continuous array sensors are more than the physical array sensors by difference method, the DFT algorithm is also extended to the DOA estimation of sparse arrays. However, the conventional DFT estimation algorithm uses the method of phase deflection to finely search the angles, whose estimation accuracy will no longer improve with the decrease of the search step when it reaches the upper limit. Reference [21] proposes an improved DFT algorithm by Taylor expansion of the expression of the co-array equivalent received signal, combined with the total least squares (TLS) method. This algorithm avoids the fine search of angle and achieves higher accuracy than the conventional DFT estimation algorithm, but the performance of this algorithm is poor under a large number of snapshots. In recent years, the algorithms based on compressed sensing is the research hotspot of DOA estimation of sparse array. Reference [22] applies OMP algorithm to DOA estimation. By dividing the over-complete redundant dictionary and using all virtual sensors of difference co-array, it gives full play to the high DOF of sparse array structure. However, the estimation accuracy of the algorithm is related to the search step. The acquisition of high estimation accuracy means more precise step, but also brings higher computational complexity.

In order to take advantage of the high estimation accuracy of the compressed sensing algorithm and avoid the increase of computational complexity caused by the fine division search step, in this paper, we propose a DOA estimation algorithm based on the sparse array that can generate large aperture difference co-array: Firstly, the low complexity DFT algorithm is used to estimate the DOA of the received signal, and the initial estimation result with large error is obtained; Then, based on the uneven distribution of data points and angle values in DFT spectrum, a basic over-complete redundant dictionary division strategy is proposed to construct a reasonable complete over-complete redundant dictionary; Finally, through an improved OMP algorithm based on the complete over-complete redundant dictionary, the final DOA estimation is obtained.

The remainder of this paper is presented as follows. Section II introduces some preliminaries. Steps of the proposed DOA estimation method are elaborated in Section III. Section IV compares and analyzes the computational complexity of various sparse array DOA estimation algorithms. Section V presents the results of the numerical simulation experiments. Section VI summarizes the whole paper.

II. PRELIMINARY

A. SPARSE ARRAY RECEIVED SIGNAL MODEL

Suppose that K independent far-field narrowband signals are received by a sparse array at the power $\{\sigma_1^2, \sigma_2^2, \ldots, \sigma_K^2\}$ from the direction of $\{\theta_1, \theta_2, \ldots, \theta_K\}$, respectively. If the array sensor position set of a sparse array is recorded as $\mathbb{D} = \{d_1, d_2, \ldots, d_M\}$, where M is the total number of array sensors, the received signal can be expressed as

$$\boldsymbol{X}(t) = \boldsymbol{A}\boldsymbol{S}(t) + \boldsymbol{N}(t), \tag{1}$$

where the array manifold matrix $\boldsymbol{A}$ can be expressed as

$$\boldsymbol{A} = [\boldsymbol{a}_{\mathbb{D}}(\theta_1), \boldsymbol{a}_{\mathbb{D}}(\theta_2), \ldots, \boldsymbol{a}_{\mathbb{D}}(\theta_K)], \tag{2}$$

$$\boldsymbol{a}_{\mathbb{D}}(\theta_k) = \left[1, e^{-j\pi d_2 \sin(\theta_k)}, \ldots, e^{-j\pi d_M \sin(\theta_k)}\right]^T. \tag{3}$$

The signal vector $\boldsymbol{S}(t)$ is

$$\boldsymbol{S}(t) = [S_1(t), S_2(t), \ldots, S_K(t)]^T, \tag{4}$$

where $t = 1, 2, \ldots, J$, J represents the snapshots.

And the noise vector $\boldsymbol{N}(t)$ is

$$\boldsymbol{N}(t) = [N_1(t), N_2(t), \ldots, N_M(t)]^T. \tag{5}$$

In AWGN channel, the noise component satisfies the Gaussian distribution with mean value 0 and variance σ_n^2.

Next, because the source signals are uncorrelated with each other and they are uncorrelated with noise, the covariance matrix $\boldsymbol{R}_X$ of the received signal is calculated by

$$\boldsymbol{R}_X = E[\boldsymbol{X}\boldsymbol{X}^H] = \boldsymbol{A}\boldsymbol{R}_S\boldsymbol{A}^H + \sigma_n^2\boldsymbol{I}_M, \tag{6}$$

where $\boldsymbol{R}_S = diag\left[\sigma_1^2, \sigma_2^2, \ldots, \sigma_K^2\right]$. The column vectorization of $\boldsymbol{R}_X$ can be obtained as

$$\boldsymbol{Z} = vec(\boldsymbol{R}_X) = (\boldsymbol{A}^* \circ \boldsymbol{A})\boldsymbol{p} + \sigma_n^2\boldsymbol{e}_n, \tag{7}$$

where $\boldsymbol{p} = [\sigma_1^2, \sigma_2^2, \ldots, \sigma_K^2]^H$, $\boldsymbol{e}_n = vec(\boldsymbol{I}_M)$. Define $\boldsymbol{B} = \boldsymbol{A}^* \circ \boldsymbol{A}$, and $\circ$ represents the Khatri-Rao product, then

$$\boldsymbol{B} = [\boldsymbol{b}(\theta_1), \boldsymbol{b}(\theta_2), \ldots, \boldsymbol{b}(\theta_K)], \tag{8}$$

$$\begin{aligned}\boldsymbol{b}(\theta_k) = [&e^{-j\pi(d_1-d_1)\sin(\theta_k)}, e^{-j\pi(d_2-d_1)\sin(\theta_k)}, \\ &\ldots, e^{-j\pi(d_m-d_n)\sin(\theta_k)}, \ldots, e^{-j\pi(d_M-d_M)\sin(\theta_k)}]^T.\end{aligned} \tag{9}$$

As a result, the position difference set of physical array sensors is defined as

$$\mathbb{D}_v = \{d_m - d_n | d_m \in \mathbb{D}, d_n \in \mathbb{D}\}. \tag{10}$$

In this case, the elements in the set $\mathbb{D}_v$ are regarded as the sensor positions of a virtual linear array, and Eq.(7) can be regarded as the received signal vector on the virtual array $\mathbb{D}_v$.

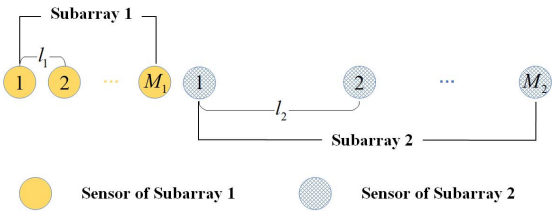

FIGURE 1. Structure of NA.

B. NESTED ARRAY

The DOA estimation method proposed in this paper is suitable for sparse arrays which can generate continuous difference co-array with large aperture. The more continuous virtual array sensors can be generated by the array, the better the DOA estimation performance of the method is. In order to facilitate the experimental simulation, the classical NA is chosen in this paper. This subsection gives a brief introduction to NA.

As shown in Figure 1, NA consists of two ULAs.

Suppose that the sensor number of two ULAs are M_1 and M_2 and the sensor spacing is l_1 and l_2, respectively. l_1 equals half-wavelength of the received signal, $l_2 = (M_1+1)l_1$. Then the set of sensor positions of NA can be expressed as

$$\begin{aligned}\mathbb{L}_{NA} &= \{m_1 l_1 | m_1 = 1, 2, \ldots, M_1\} \\ &\cup \{m_2 l_2 | m_2 = 1, 2, \ldots, M_2\}. \end{aligned} \tag{11}$$

According to [13], for an NA with total sensor number equals to M, the optimal array arrangement and the available difference co-array aperture size are shown in Table 1.

TABLE 1. Sub-array sensor numbers and difference co-array aperture size of the *M*-sensor NA.

M	Sub-array sensor numbers	difference co-array aperture size
odd	$M_1 = \frac{M-1}{2}, M_2 = \frac{M+1}{2}$	$\frac{M^2-1}{2} + M$
even	$M_1 = M_2 = \frac{M}{2}$	$\frac{M^2-2}{2} + M$

C. CRAMER-RAO BOUND OF SPARSE ARRAY DOA ESTIMATION

The Cramer-Rao Bound (CRB) of sparse array DOA estimation has been fully studied and discussed in many existing literatures. According to [23], [24], it can be expressed as:

$$CRB_\theta = \frac{1}{N}(\boldsymbol{M}_\theta^H \boldsymbol{\Pi}_{\boldsymbol{M}_S}^{\perp} \boldsymbol{M}_\theta)^{-1}, \tag{12}$$

where,

$$\boldsymbol{M}_\theta = (\boldsymbol{R}^T \otimes \boldsymbol{R})^{-\frac{1}{2}} \dot{\boldsymbol{A}}_d \boldsymbol{P}, \tag{13}$$

$$\boldsymbol{M}_S = (\boldsymbol{R}^T \otimes \boldsymbol{R})^{-\frac{1}{2}} \left[\dot{\boldsymbol{A}}_d \ \boldsymbol{i}\right], \tag{14}$$

$$\boldsymbol{\Pi}_{\boldsymbol{M}_S}^{\perp} = \boldsymbol{I} - \boldsymbol{M}_S(\boldsymbol{M}_S^H \boldsymbol{M}_S)^{-1} \boldsymbol{M}_S^H, \tag{15}$$

and,

$$\dot{\boldsymbol{A}}_d = \dot{\boldsymbol{A}}^* \odot \boldsymbol{A} + \boldsymbol{A}^* \odot \dot{\boldsymbol{A}}, \tag{16}$$

$$\dot{\boldsymbol{A}} = \left[\frac{\partial \boldsymbol{a}(\theta_1)}{\theta_1}, \frac{\partial \boldsymbol{a}(\theta_2)}{\theta_2}, \ldots, \frac{\partial \boldsymbol{a}(\theta_K)}{\theta_K}\right]. \tag{17}$$

Based on the above, the CRB of DOA estimation using sparse array can be easily obtained.

III. THE PROPOSED DOA ESTIMATION METHOD

The DOA estimation method proposed in this paper firstly performs DFT on the received signal of the equivalent continuous difference co-array obtained by vectorizing the covariance matrix of the received signal to acquire the initial estimated value of DOA; secondly, within a small angle range around each initial estimated value construct a basic over-complete redundant dictionary, and combine all the obtained basic over-complete redundanct dictionaries to form a complete over-complete redundant dictionary; finally, based on the received signal of the equivalent difference co-array, an improved OMP algorithm is used to fine-search the angles, and the final DOA estimation results are obtained. The flow of proposed method is as follows.

A. DOA INITIAL ESTIMATION BASED ON DFT

The equivalent received signal of the continuous difference co-array part is intercepted from the difference co-array equivalent received signal $\boldsymbol{Z}$ obtained from Eq.(7) to acquire the vector $\boldsymbol{Z}_1$, which is expressed as

$$\boldsymbol{Z}_1 = \tilde{\boldsymbol{B}}\boldsymbol{p} + \sigma_n^2 \tilde{\boldsymbol{e}}_n. \tag{18}$$

where, $\tilde{\boldsymbol{e}}_n$ is the noise corresponding to the equivalent signal received by the continuous difference co-array, and the array manifold matrix $\tilde{\boldsymbol{B}}$ is

$$\tilde{\boldsymbol{B}} = [\tilde{\boldsymbol{b}}(\theta_1), \tilde{\boldsymbol{b}}(\theta_2), \ldots, \tilde{\boldsymbol{b}}(\theta_K)], \tag{19}$$

$$\tilde{\boldsymbol{b}}(\theta_k) = [1, e^{-j\pi d \sin\theta_k/\lambda}, \ldots, e^{-j\pi(T_c-1)d\sin\theta_k/\lambda}]^T, \tag{20}$$

where, d is the sensor spacing of the continuous difference co-array, which is equal to half the wavelength λ of the signal received by the array, and T_c is the sensor number of the continuous difference co-array. Therefore, $\tilde{\boldsymbol{b}}(\theta_k)$ can be reduced to

$$\tilde{\boldsymbol{b}}(\theta_k) = [1, e^{-j\pi \sin\theta_k}, \ldots, e^{-j\pi(T_c-1)\sin\theta_k}]^T. \tag{21}$$

The normalized matrix $\boldsymbol{F}$ of DFT is expressed as

$$\boldsymbol{F} = \frac{1}{\sqrt{T_c}} \begin{bmatrix} W_{T_c}^{1} & W_{T_c}^{2} & \ldots & W_{T_c}^{T_c} \\ W_{T_c}^{2} & W_{T_c}^{1} & \ldots & W_{T_c}^{2T_c} \\ \ldots & \ldots & \ldots & \ldots \\ W_{T_c}^{T_c} & W_{T_c}^{2T_c} & \ldots & W_{T_c}^{{T_c}^2} \end{bmatrix}, \tag{22}$$

where the element of the p-th row and q-th column is $W_{T_c}^{pq} = e^{-j\frac{2\pi}{T_c}pq}$.

$\tilde{\boldsymbol{\beta}}(\theta_k)$ can be obtained by DFT of array flow pattern vector $\tilde{\boldsymbol{b}}(\theta_k)$, which is expressed as

$$\tilde{\boldsymbol{\beta}}(\theta_k) = \boldsymbol{F}\tilde{\boldsymbol{b}}(\theta_k). \tag{23}$$

where the q-th element is

$$[\tilde{\boldsymbol{\beta}}(\theta_k)]_q = \frac{\sin[\frac{T_c}{2}(\frac{2\pi}{T_c}q+\pi\sin\theta_k)]e^{-j\frac{T_c-1}{2}(\frac{2\pi}{T_c}q+\pi\sin\theta_k)}}{\sqrt{T_c}\sin[\frac{1}{2}(\frac{2\pi}{T_c}q+\pi\sin\theta_k)]}. \quad (24)$$

It can be seen from Eq.(24) that only when $q_k = -T_c\sin\theta_k/2$ is an integer, $\tilde{\boldsymbol{\beta}}(\theta_k)$ has and only the q_k-th element is not zero, then all the power of the signal is concentrated at the q_k-th point of the DFT spectrum, and the DOA estimation of θ_k can be obtained directly from the position of that point.

However, in practice, q_k is not an integer in most cases, and the signal power will be leaked from the $(-T_c\sin\theta_k/2)$-th point to the surrounding points and it will appear on the DFT spectrum that several elements adjacent to q_k are not zero, and the remaining elements are close to zero. Therefore, the θ_k can be initially estimated by finding the peak position q_k of the non-zero elements in $\tilde{\boldsymbol{\beta}}(\theta_k)$.

Since the angles of source signals are unknown quantities, the array flow pattern vector $\tilde{\boldsymbol{b}}(\theta_k)$ cannot be obtained directly, and the angles estimation can only be obtained by performing DFT transformation on $\boldsymbol{Z}_1$. Assuming that $\boldsymbol{y} = \boldsymbol{F}\boldsymbol{Z}_1$ is obtained by performing DFT transformation on the equivalent received signal of the continuous difference co-array. The positions of the large peaks are found in the DFT spectrum, which are marked as $\tilde{q}_k$, and the number of the peaks equal to the source signal number K. Then the initial DOA estimation is expressed as

$$\tilde{\theta}_k = \arcsin(-2\tilde{q}_k/T_c), \quad k = 1, 2, \ldots, K. \quad (25)$$

B. OVER-COMPLETE REDUNDANT DICTIONARY DIVISION STRATEGY

Because the corresponding angle difference between any point in the DFT spectrum and its previous point and the corresponding angle difference between this point and its latter point are not equal, a simple average allocation strategy cannot be adopted to determine the range of the basic over-complete redundant dictionaries around the initial estimation angles. In this section, a division strategy of over-complete redundant dictionary is designed as follows.

It is known that the peak position of the k-th angle of source signals is $\tilde{q}_k$. Take the two adjacent locations $\tilde{q}_k - 1$ and $\tilde{q}_k + 1$ and calculate their corresponding angles, which are recorded as

$$\begin{cases} \phi_k = \arcsin[-2(\tilde{q}_k - 1)/T_c] \\ \psi_k = \arcsin[-2(\tilde{q}_k + 1)/T_c]. \end{cases} \quad (26)$$

Then, the range of the basic over-complete redundant dictionary obtained by $\tilde{\theta}_k$ is $[\frac{\tilde{\theta}_k+\phi_k}{2}, \frac{\tilde{\theta}_k+\psi_k}{2}]$. By combining K basic over-complete redundant dictionaries, the complete over-complete redundant dictionary needed for accurate estimation is obtained as

$$\Theta_G = \{[\frac{\tilde{\theta}_1+\phi_1}{2}, \frac{\tilde{\theta}_1+\psi_1}{2}], [\frac{\tilde{\theta}_2+\phi_2}{2}, \frac{\tilde{\theta}_2+\psi_2}{2}], \ldots, [\frac{\tilde{\theta}_k+\phi_k}{2}, \frac{\tilde{\theta}_k+\psi_k}{2}], \ldots, [\frac{\tilde{\theta}_K+\phi_K}{2}, \frac{\tilde{\theta}_K+\psi_K}{2}]\}. \quad (27)$$

where G denotes the number of elements in complete over-complete redundant dictionary. Because the range of each basic over-complete redundant dictionary varies, it can be known that the number of elements in them may be different. Then, the Θ_G can be abbreviated as

$$\Theta_G = \{\dot{\theta}_1, \dot{\theta}_2, \ldots, \dot{\theta}_G\}. \quad (28)$$

C. ACCURATE ESTIMATION BASED ON IMPROVED OMP ALGORITHM

The extended flow pattern matrix $\boldsymbol{A}_{\Theta_G}$ is constructed according to Θ_G, that is,

$$\begin{aligned} \boldsymbol{A}_{\Theta_G} &= \{\boldsymbol{a}_{\mathbb{D}_v}(\dot{\theta}_1), \boldsymbol{a}_{\mathbb{D}_v}(\dot{\theta}_2), \ldots, \boldsymbol{a}_{\mathbb{D}_v}(\dot{\theta}_G)\} \\ &= \{\boldsymbol{e}^{-j2\pi\boldsymbol{d}_v\sin\dot{\theta}_1/\lambda}, \boldsymbol{e}^{-j2\pi\boldsymbol{d}_v\sin\dot{\theta}_2/\lambda}, \ldots, \boldsymbol{e}^{-j2\pi\boldsymbol{d}_v\sin\dot{\theta}_G/\lambda}\}. \end{aligned} \quad (29)$$

where $\boldsymbol{d}_v$ is a column vector indicating the position of difference co-array sensors. The signal model shown in Eq.(7) can be transformed into a sparse representation problem, that is,

$$\boldsymbol{Z} = \boldsymbol{A}_{\Theta_G}\boldsymbol{p}_\Theta + \sigma_n^2\boldsymbol{e}_n. \quad (30)$$

where $\boldsymbol{p}_\Theta \in \mathbb{R}^{G\times 1}$ is a sparse vector with sparse degree K. If there are source signals incident in the $\theta_g(g = 1, 2, \ldots, G)$ direction, then the g-th element of $\boldsymbol{p}_\Theta$ is $p_g \neq 0$, otherwise $p_g = 0$.

Taylor expansion is performed on $\boldsymbol{a}_{\mathbb{D}_v}(\dot{\theta}_k)$, when the search step is small, its higher-order term can be ignored, then

$$\boldsymbol{a}_{\mathbb{D}_v}(\dot{\theta}_k) = \boldsymbol{a}_{\mathbb{D}_v}(\varphi_k) + \frac{\partial\boldsymbol{a}_{\mathbb{D}_v}(\varphi_k)}{\partial\varphi_k}\Delta_{\varphi_k}, \quad (31)$$

where $\Delta_{\varphi_k} = \dot{\theta}_k - \varphi_k$. Therefore, $\boldsymbol{A}_{\Theta_G}$ can be expressed as

$$\begin{aligned} \boldsymbol{A}_{\Theta_G} &= \boldsymbol{A}_{\Theta_G}(\varphi) + \frac{\partial\boldsymbol{A}_{\Theta_G}(\varphi)}{\partial\varphi}\boldsymbol{\Delta}_\varphi \\ &= \boldsymbol{A}_{\Theta_G}(\varphi) + \boldsymbol{\chi}_\varphi\boldsymbol{\Delta}_\varphi, \end{aligned} \quad (32)$$

where

$$\boldsymbol{\Delta}_\varphi = diag\{\dot{\theta}_1 - \varphi_1, \dot{\theta}_2 - \varphi_2, \ldots, \dot{\theta}_G - \varphi_G\}. \quad (33)$$

Let $\boldsymbol{p}_\Theta^\varphi = \boldsymbol{\Delta}_\varphi\boldsymbol{p}_\Theta$, then Eq.(30) can be approximately expressed as

$$\boldsymbol{Z} = \boldsymbol{A}_{\Theta_G}(\varphi)\boldsymbol{p}_\Theta + \boldsymbol{\chi}_\varphi\boldsymbol{p}_\Theta^\varphi + \sigma_n^2\boldsymbol{e}_n. \quad (34)$$

Therefore, a sparse reconstruction problem can be obtained as

$$\begin{aligned} &\min_{\boldsymbol{v},\sigma_n^2} \parallel \boldsymbol{v} \parallel_{1,2} \\ &s.t. \boldsymbol{Z} = \boldsymbol{A}_{\Theta_G}(\varphi)\boldsymbol{p}_\Theta + \boldsymbol{\chi}_\varphi\boldsymbol{p}_\Theta^\varphi + \sigma_n^2\boldsymbol{e}_n, \end{aligned} \quad (35)$$

where $\boldsymbol{v} = [\boldsymbol{p}_\Theta, \boldsymbol{p}_\Theta^\varphi]$.This problem can be solved by the OMP algorithm and its specific solving steps are as follows.

***Step* 1**: Initialize $\boldsymbol{r}_0 = \boldsymbol{Z}$, $\boldsymbol{A}_{\Theta_G}^0 = \boldsymbol{A}_{\Theta_G}$, $\boldsymbol{\chi}_{\varphi_0} = \boldsymbol{\chi}_\varphi$and sparsity K, index value set $\Omega = \oslash$, iteration times $i = 1$;

***Step* 2**: Calculate $\boldsymbol{u} = \boldsymbol{A}_{\Theta_k} \bullet \boldsymbol{r}_{i-1}$ and store the index value corresponding to the maximum value in $\boldsymbol{u}$ into Ω in the i-th iteration;

***Step* 3**: Take the columns corresponding to the index values of $\boldsymbol{A}_{\Theta_G}$ and $\boldsymbol{\chi}_{\varphi}$ to obtain $\boldsymbol{A}_{\Theta_G}^{\Omega}$ and $\boldsymbol{\chi}_{\varphi}^{\Omega}$;

***Step* 4**: Calculate $\boldsymbol{\mu}_i = ([\boldsymbol{p}_{\Theta}, \boldsymbol{p}_{\Theta}^{\varphi}, \boldsymbol{e}_n])^{\dagger}\boldsymbol{Z}$;

***Step* 5**: Update $\boldsymbol{r}_i = \boldsymbol{Z} - [\boldsymbol{p}_{\Theta}, \boldsymbol{p}_{\Theta}^{\varphi}, \boldsymbol{e}_n]\boldsymbol{\mu}_i$;

***Step* 6**: If $i < K$, set $i = i + 1$ and return to ***Step* 2**; Otherwise, stop iteration and obtain sparse vector $\boldsymbol{\mu}_K$.

$\boldsymbol{\mu}_K$ represents the estimated value of theoretical sparse vector and noise power, which can be expressed as

$$\boldsymbol{\mu}_K = [(\hat{\boldsymbol{p}}_{\Theta})^T, (\hat{\boldsymbol{p}}_{\Theta}^{\varphi})^T, \hat{\sigma}_n^2]^T. \tag{36}$$

Its first K elements are $\hat{\boldsymbol{p}}_{\Theta} = \{\hat{p}_{\Theta}^1, \hat{p}_{\Theta}^2, \ldots, \hat{p}_{\Theta}^K\}$, and the $K+1$ to $2K$ elements are $\hat{\boldsymbol{p}}_{\Theta}^{\varphi} = \{\hat{p}_{\Theta}^{\varphi_1}, \hat{p}_{\Theta}^{\varphi_2}, \ldots, \hat{p}_{\Theta}^{\varphi_K}\}$. Then, the estimation result of the modified value of the estimation of the k-th angle of DOA is

$$\hat{\Delta}_{\varphi_k} = \hat{p}_{\Theta}^{\varphi_k} / \hat{p}_{\Theta}^{k}. \tag{37}$$

The angle value in the over-complete redundant dictionary corresponding to the k-th angle of arrival can be determined by the k-th element in the set of index values Ω, that is

$$\hat{\varphi}_k = \Theta_G(\Omega_k). \tag{38}$$

Therefore, the accurate estimation result of the k-th angle of arrival based on the improved OMP algorithm is

$$\hat{\theta}_k = \hat{\varphi}_k + \hat{\Delta}_{\phi_k}. \tag{39}$$

As mentioned above, this is the flow of the DOA estimation method proposed in this paper. Compared with the Conventional DFT method using phase deflection for fine search, the proposed method has higher estimation accuracy because of the using of improved OMP method. Compared with the estimation method based on spatial smoothing, since the array aperture loss caused by spatial smoothing is avoided, the proposed method has higher estimation accuracy due to the use of all virtual sensors of difference co-array. Compared with the direct OMP method that divides the searching grids in all directions, the proposed method further estimates the results of grid search through Taylor expansion, and improves the accuracy of the estimation results. Compared with the improved DFT method proposed in [21], the proposed method can be infinitely close to the actual source signal angles by dividing a finer search grid with no upper limit. In a word, by using the DFT spectrum of the signal for initial estimation and using the OMP algorithm based on Taylor expansion for accurate estimation, the proposed method has some advantages in estimation accuracy compared with the other methods.

IV. ANALYSIS OF COMPUTATIONAL COMPLEXITY

In this section, the number of complex multiplication times is used as the evaluation standard, and the computational complexity of the conventional DFT estimation algorithm, the OMP algorithm, the SS-ESPRIT algorithm, the improved DFT algorithm proposed in the [21] and the algorithm proposed in this paper are analyzed.

Suppose that the number of physical sensors of the sparse array is M, the length of the equivalent difference co-array is T, the length of its continuous part is T_c, the source number of received signal by the array is K, the snapshots of received data is J, and the search time of algorithms using searching mrthod is G.

The mentioned algorithms are all based on the virtualization of signal covariance matrix, and the complex multiplication times of the process of calculating covariance matrix are M^2J; The complex multiplication times of the equivalent received signal of the continuous difference co-array by DFT transform are T_c^2; The complex multiplication times of fine search using phase rotation method are KGT_c; The complex multiplication times of fine search using the method of the improved DFT algorithm proposed in [21] are $(8K^2+2K)T_c$; The complex multiplication times for using the SS-ESPRIT algorithm to estimate the DOA of the continuous difference co-array equivalent received signal are $(T_c+1)^3/4 + 2(T_c+1)K^2 + 11K^3$; The complex multiplication times in the iterative process of solving DOA by OMP algorithm are $KGT + K(K+1)[K(K+1)/4 + 2(K+2)T/3]$; The complex multiplication times of fine search using the method of the proposed algorithm in this paper are $KGT + K(K+1)[2K(K+3) + (8K+10)T/3 + 9] + T + 1$. Therefore, the computational complexity expressions of each algorithm are shown in Table 2.

TABLE 2. Computational Complexity Expressions for Different Estimation Algorithms.

Algorithm	Computational Complexity
Conventional DFT	$\mathcal{O}(M^2J + T_c^2 + KGT_c)$
Improved DFT	$\mathcal{O}(M^2J + T_c^2 + (8K^2 + 2K)T_c)$
OMP	$\mathcal{O}(M^2J + KGT + K(K+1)[K(K+1)/4 + 2(K+2)T/3])$
SS-ESPRIT	$\mathcal{O}(M^2J + (T_c+1)^3/4 + 2(T_c+1)K^2 + 11K^3)$
Proposed	$\mathcal{O}(M^2J + KGT + K(K+1)[2K(K+3) + (8K+10)T/3 + 9] + T + 1)$

In the case of comprehensively considering the search accuracy and computational complexity of each grid search algorithm, the search times of the conventional DFT algorithm are set to $G = 180$ and $G = 900$, the search times of the OMP algorithm are set to $G = 1800$, and the search times of the algorithm proposed in this paper are set to $G = 180$. Using a 17-sensor NA, the estimated sources number K varies from 1 to 30, and when the snapshots J is 2000, the computational complexity of each DOA estimation algorithm is varying as shown in Figure 2.

As can be seen from Figure 2, the computational complexity of the proposed algorithm increases exponentially with the increase of the source number. When the source number is

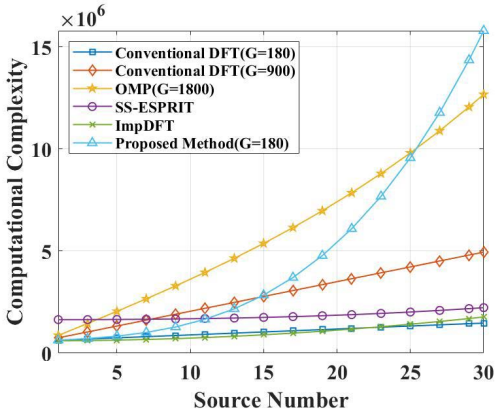

FIGURE 2. Variation of Computational Complexity of Different Algorithms with Source Numbers.

much less than sensor number ($K < 11$), the computational complexity of the proposed algorithm is at a low level, which is only higher than the conventional DFT algorithm with 180 search times and the improved DFT algorithm proposed in [21]. When the source number is close to sensor number ($11 \leq K < 17$), the computational complexity of the proposed algorithm is higher than that of the SS-ESPRIT algorithm and is gradually close to the conventional DFT algorithm with 900 search times. When the source number exceeds sensor number ($K \geq 17$), the computational complexity of the proposed algorithm increases rapidly and gradually surpasses the OMP algorithm with 1800 search times.

V. NUMERICAL SIMULATION EXPERIMENTS

In order to verify the performance of the proposed DOA estimation algorithm, based on the classical NA introduced in Section II, simulation experiments are carried out to compare the proposed algorithm with the conventional DFT algorithm, the OMP algorithm, the improved DFT algorithm proposed in [21] and the SS-ESPRIT algorithm.

A. SUCCESS RATE OF DOA ESTIMATION

One of the advantages of sparse array over ULA is that it can achieve underdetermined estimation. DOA estimation algorithm needs to make full use of its underdetermined estimation ability. This subsection compares and simulates the success rate of signal DOA estimation of each algorithm.

Simulation parameters: 17-sensor NA, snapshots $J = 2000$, $SNR = 5dB$, the source number K varies from 1 to 56 at intervals of 5, the elements of arrival angle vector $\boldsymbol{\theta}$ is uniformly distributed in the range of $[-60°, 60°]$, the search times G of search class algorithms are set according to the parameters in Section IV, and Monte Carlo simulation times B is 200.

In this paper, the conditions for judging the success of a single DOA estimation are set as

$$\Delta\theta_k = \frac{1}{K}\sum_{k=1}^{K}|\hat{\theta}_k - \theta_k| \leq 0.05°. \tag{40}$$

If the number of experiments in which DOA estimation is successfully realized in B Monte Carlo experiments is recorded as C, then the success rate of estimation is $r_s = C/B$.

According to the above simulation parameters, the results that the estimated success rate of each algorithm varies with source number is shown in Figure 3.

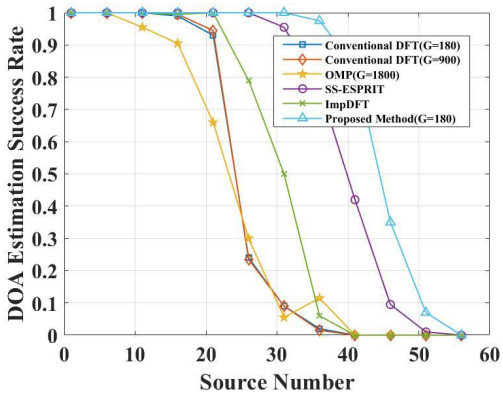

FIGURE 3. Variation of Success Rate of DOA Estimation with Different Algorithms with Source Numbers.

The simulation results show that the DOA estimation success rate of the proposed algorithm is significantly better than that of other comparison algorithms, indicating that the proposed algorithm can give full play to the aperture advantage of sparse arrays and achieve DOA estimation of more targets.

B. ROOT MEAN SQUARE ERROR

This subsection presents the Root Mean Square Error (RMSE) of DOA estimation results of various algorithms under different source number. This paper uses the definition of RMSE as

$$RMSE = \sqrt{\frac{1}{KB}\sum_{k=1}^{K}\sum_{b=1}^{B}[(\hat{\theta}_{k,l} - \theta_k)^2]}, \tag{41}$$

where, K represents the source number, B is the Monte Carlo simulation times, the estimated angle of the k-th source during the b-th Monte Carlo simulation is expressed as $\hat{\theta}_{k,b}$ and θ_k represents the actual angle of the k-th source.

From the complexity analysis results of section IV, it can be seen that when the relationship between the source number and the sensor number changes, the relationship between the computational complexity of the proposed algorithm and other algorithms is also constantly changing. In this section, by setting different parameters of source number, the DOA estimation performance of the proposed algorithm is verified by simulation.

1) DOA ESTIMATION WHEN SOURCE NUMBER IS MUCH FEWER THAN SENSOR NUMBER

According to Figure 2, when source number is much fewer than sensor number, the computational complexity of the proposed algorithm is only higher than that of the conventional

DFT algorithm with 180 search times and the improved DFT algorithm proposed in [21]. Therefore, the computational complexity of each algorithm and the RMSEs of the DOA estimation results vary with SNR and snapshots, as shown in Figures 4, 5 and 6.

Simulation parameters: 17-sensor NA, source number $K = 9$, the elements of arrival angle vector $\boldsymbol{\theta}$ is uniformly distributed in the range of $[-60°, 60°]$, the search times G of search class algorithms are set according to the parameters in section IV. According to Table 2, in the computational complexity expressions of different algorithms, the snapshots J only exists in the computational complexity of the covariance matrix process $\mathcal{O}(M^2J)$, and the value of this item is equal in the expressions of all algorithms. Therefore, the value of the snapshots J does not affect the comparison of computational complexity, so the snapshot is taken as a fixed value, which is the same in the subsequent simulation and will not be described again.

(1) Parameters for computational complexity: $SNR = 5dB$, snapshots $J = 2000$.

(2) Parameters for RMSE vs. SNR: SNR varies from -10dB to 16dB at 2dB intervals, snapshots $J = 2000$, Monte Carlo simulation times $B = 200$.

(3) Parameters for RMSE vs. snapshots: snapshots $J = [20, 50, 100, 500, 1000, 2000, 3000, 4000, 5000]$, $SNR = 5dB$, Monte Carlo simulation times $B = 200$.

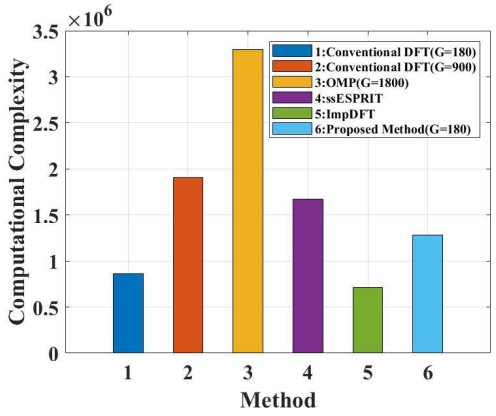

FIGURE 4. Computational Complexity of Different Algorithms with Source Numbers $K = 9$.

The simulation results show that when source number is much fewer than sensor number, the computational complexity of the proposed algorithm is low, but its DOA estimation accuracy is higher than that of the other algorithms.

2) DOA ESTIMATION WHEN SOURCE NUMBER IS CLOSE TO SENSOR NUMBER

According to Figure 2, when source number is close to sensor number, computational complexity of the proposed algorithm is higher than that of the SS-ESPRIT algorithm and close to the traditional DFT algorithm with 900 search times.

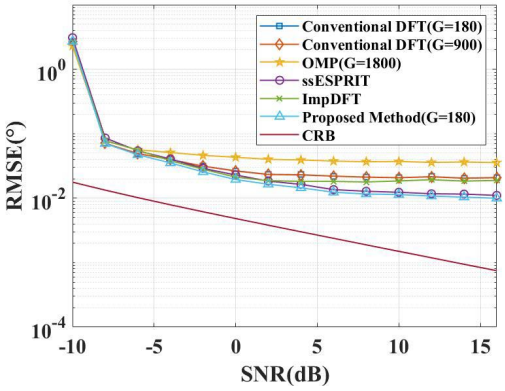

FIGURE 5. Variation of RMSE for Different Algorithms with SNR, when Source Number $K = 9$.

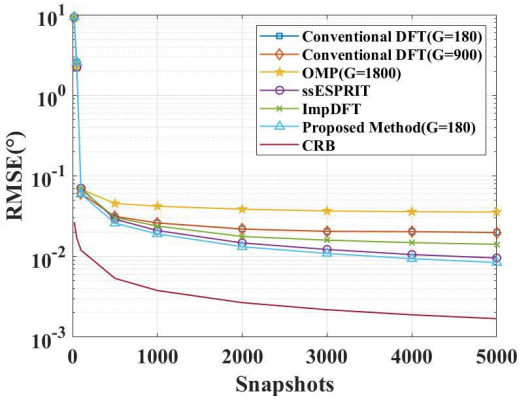

FIGURE 6. Variation of RMSE for Different Algorithms with Snapshots, when Source Number $K = 9$.

Therefore, the computational complexity of each algorithm and the RMSEs of the DOA estimation results vary with SNR and snapshots, as shown in Figures 7, 8 and 9.

Simulation parameters: 17-sensor NA, source number $K = 15$, the elements of arrival angle vector $\boldsymbol{\theta}$ is uniformly distributed in the range of $[-60°, 60°]$, the search times G of search class algorithms are set according to the parameters in section IV.

(1) Parameters for computational complexity: $SNR = 5dB$, snapshots $J = 2000$.

(2) Parameters for RMSE vs. SNR: SNR varies from -10dB to 16dB at 2dB intervals, snapshots $J = 2000$, Monte Carlo simulation times $B = 200$.

(3) Parameters for RMSE vs. snapshots: snapshots $J = [20, 50, 100, 500, 1000, 2000, 3000, 4000, 5000]$, $SNR = 5dB$, Monte Carlo simulation times $B = 200$.

The simulation results show that the computational complexity of the proposed algorithm increases when source number is close to sensor number, and the DOA estimation accuracy of the proposed algorithm is a little lower than that of other algorithms under low SNR and few snapshots, but the estimation accuracy of the proposed algorithm is still the highest under most conditions.

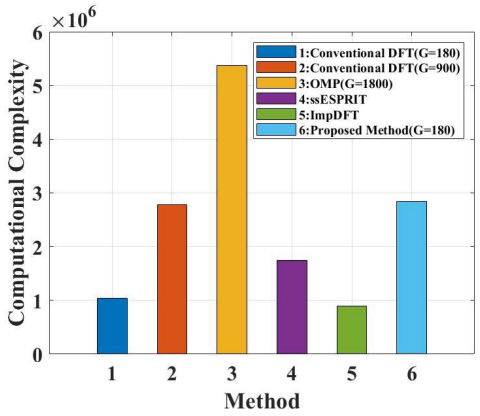

FIGURE 7. Computational Complexity of Different Algorithms with Source Numbers $K = 15$.

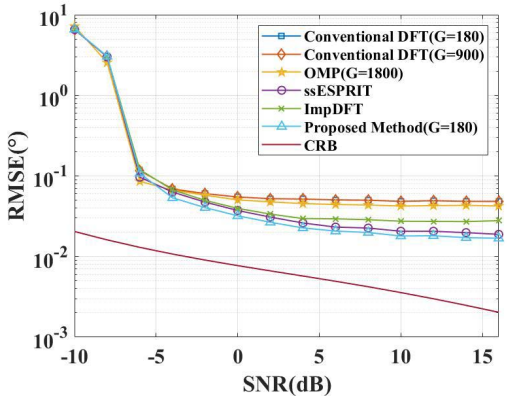

FIGURE 8. Variation of RMSE for Different Algorithms with SNR, when Source Number $K = 15$.

3) DOA ESTIMATION WHEN SOURCE NUMBER EXCEEDS SENSOR NUMBER

According to Figure 2, when source number exceeds sensor number, the computational complexity of the proposed algorithm is higher than that of the SS-ESPRIT algorithm and close to the conventional DFT algorithm with 900 search times. Therefore, the computational complexity of each algorithm and the RMSEs of the DOA estimation results vary with SNR and snapshots, as shown in Figures 10, 11 and 12.

Simulation parameters: 17-sensor NA, source number $K = 15$, the elements of arrival angle vector $\boldsymbol{\theta}$ is uniformly distributed in the range of $[-60°, 60°]$, the search times G of search class algorithms are set according to the parameters in section IV.

(1) Parameters for computational complexity: $SNR = 5dB$, snapshots $J = 2000$.

(2) Parameters for RMSE vs. SNR: SNR varies from -10dB to 16dB at 2dB intervals, snapshots $J = 2000$, Monte Carlo simulation times $B = 200$.

(3) Parameters for RMSE vs. snapshots: snapshots $J = [20, 50, 100, 500, 1000, 2000, 3000, 4000, 5000]$, $SNR = 5dB$, Monte Carlo simulation times $B = 200$.

The simulation results show that when source number exceeds sensor number, the computational complexity of the proposed algorithm is much higher than that of the other algorithms, and the DOA estimation accuracy of the proposed algorithm is worse than that of SS-ESPRIT algorithm and OMP algorithm when the SNR is low as well as the snapshots are few; when the SNR is high and the snapshots are many, the DOA estimation accuracy of the proposed algorithm is better than that of the other algorithms.

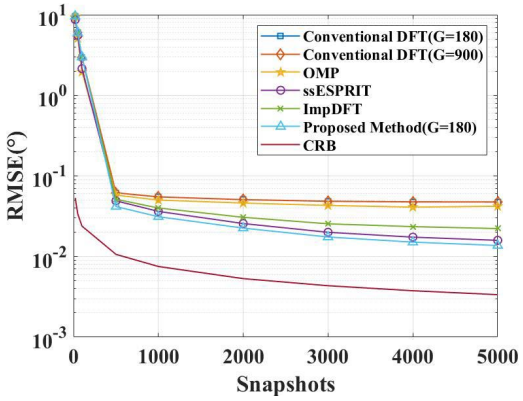

FIGURE 9. Variation of RMSE for Different Algorithms with Snapshots, when Source Number $K = 15$.

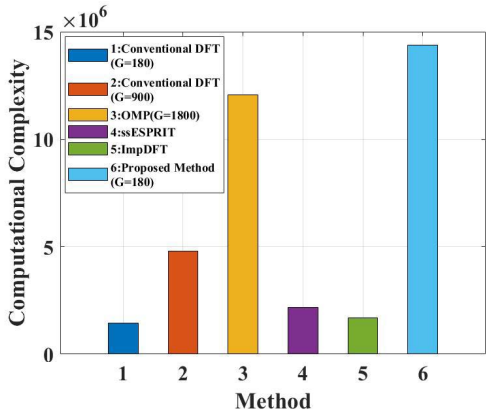

FIGURE 10. Computational Complexity of Different Algorithms with Source Numbers $K = 29$.

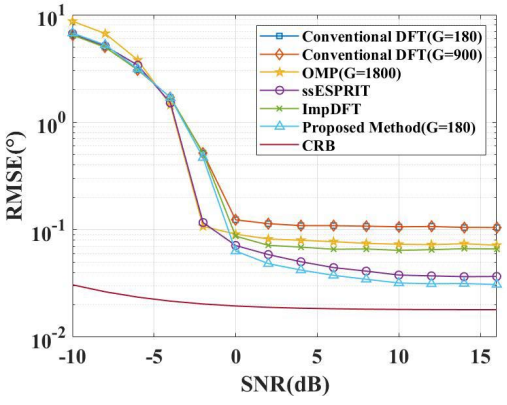

FIGURE 11. Variation of RMSE for Different Algorithms with SNR, when Source Number $K = 29$.

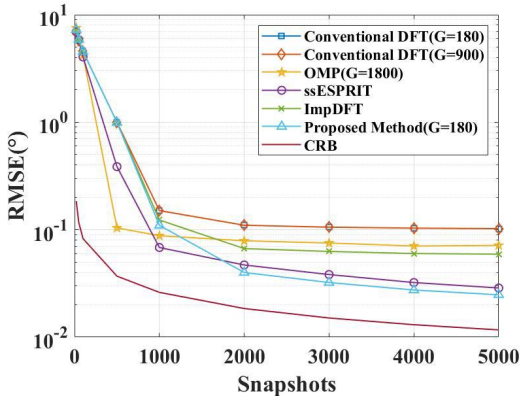

FIGURE 12. Variation of RMSE for Different Algorithms with Snapshots, when Source Number $K = 29$.

Through a comprehensive analysis of the above three groups of comparative simulation experiments, we can draw the following conclusions: compared with the traditional DFT algorithm, OMP algorithm, SS-ESPRIT algorithm and the improved DFT algorithm proposed in [21], the proposed algorithm can achieve relatively higher DOA estimation accuracy under the condition that the source number is close to or fewer than the sensor number. When the source number increases, the DOA estimation accuracy of the proposed algorithm will be lower than that of SS-ESPRIT and OMP algorithms under low SNR and few snapshots. The reason for the above phenomenon is that in order to reduce the complexity caused by search times, the proposed algorithm initially estimates the angles by calculating the DFT spectrum of the equivalent received signal. The number of sources that this method can distinguish is limited by the length of the array, and under low SNR and few snapshots, the DFT spectrum will produce more pseudo-peaks, which will affect the result of DOA estimation. Therefore, the traditional DFT algorithm and the improved DFT algorithm proposed in [21] are also affected by low SNR and few snapshots, while SS-ESPRIT and OMP algorithms that do not use DFT for initial estimation are not significantly affected by low SNR and few snapshots.

VI. CONCLUSION

In this paper, aiming at the problem of signal DOA estimation of sparse array, based on the large aperture continuous difference co-array generated by sparse array, a high precision DOA estimation algorithm is proposed. After the initial estimation result is obtained by using the DFT spectrum, the over-complete redundant dictionary is divided according to the initial estimation angles. Finally, the accurate DOA estimation result is obtained by using the improved OMP algorithm. The simulation results show that, compared with the conventional DFT algorithm, the improved DFT algorithm, the OMP algorithm and the SS-ESPRIT algorithm, the proposed algorithm can give full play to the large aperture advantage of sparse array and achieve the DOA estimation of more sources, and the proposed algorithm has higher estimation accuracy when the snapshots are many and the SNR is high.

However, due to the limitation of DFT, the estimation accuracy of the proposed algorithm will be affected under the conditions of large number of sources, few snapshots and low SNR. Subsequently, the estimation performance of the proposed algorithm can be further improved by improving the accuracy of the initial estimation.

REFERENCES

[1] R. Cao, S. Liu, Z. Mao, and Y. Huang, "Doubly-toeplitz-based interpolation for joint DoA-range estimation using coprime FDA," in *Proc. IEEE Radar Conf. (RadarConf21)*, May 2021, pp. 1–6, doi: 10.1109/RadarConf2147009.2021.9455275.

[2] F. Sun, Q. Wu, P. Lan, G. Ding, and L. Chen, "Real-valued DOA estimation with unknown number of sources via reweighted nuclear norm minimization," *Signal Process.*, vol. 148, pp. 48–55, Jul. 2018, doi: 10.1016/j.sigpro.2018.02.014.

[3] L. Zhang, J. Mei, A. Zielinski, and P. Cai, "Direction-of-arrival estimation for far-field acoustic signal in presence of near-field interferences," *Electron. Lett.*, vol. 51, no. 1, pp. 101–103, 2015, doi: 10.1049/el.2014.1847.

[4] J. Yang, Y. Yang, J. Lu, and L. Yang, "Iterative methods for DOA estimation of correlated sources in spatially colored noise fields," *Signal Process.*, vol. 185, pp. 100–108, Aug. 2021, doi: 10.1016/j.sigpro.2021.108100.

[5] R. O. Schmidt, "Multiple emitter location and signal parameter estimation," *IEEE Trans. Antennas Propag.*, vol. AP-34, no. 3, pp. 276–280, Mar. 1986, doi: 10.1109/TAP.1986.1143830.

[6] R. Roy and T. Kailath, "Esprit-estimation of signal parameters via rotational invariance techniques," *IEEE Trans. Acoust., Speech, Signal Process.*, vol. 37, no. 7, pp. 984–995, Jul. 1989, doi: 10.1109/29.32276.

[7] S. Marcos, A. Marsal, and M. Benidir, "The propagator method for source bearing estimation," *Signal Process.*, vol. 42, no. 2, pp. 121–138, 1995, doi: 10.1016/0165-1684(94)00122-G.

[8] B. D. Rao and K. V. S. Hari, "Performance analysis of root-music," *IEEE Trans. Acoust., Speech, Signal Process.*, vol. 37, no. 12, pp. 1939–1949, Dec. 1989, doi: 10.1109/29.45540.

[9] R. Roy, A. Paulraj, and T. Kailath, "ESPRIT–A subspace rotation approach to estimation of parameters of cisoids in noise," *IEEE Trans. Acoust., Speech, Signal Process.*, vol. ASSP-34, no. 5, pp. 1340–1342, Oct. 1986, doi: 10.1109/TASSP.1986.1164935.

[10] Y. Yang, X. Mao, G. Jiang, and Y. Wang, "Spatially separated nested vector-sensor array with reduced mutual coupling," *IEEE Sensors J.*, vol. 19, no. 14, pp. 5801–5817, Jul. 2019, doi: 10.1109/JSEN.2019.2905148.

[11] J. He, L. Li, and T. Shu, "2-D direction finding using parallel nested arrays with full co-array aperture extension," *Signal Process.*, vol. 178, Jan. 2021, Art. no. 107795, doi: 10.1016/j.sigpro.2020.107795.

[12] A. Moffet, "Minimum-redundancy linear arrays," *IEEE Trans. Antennas Propag.*, vol. AP-16, no. 2, pp. 172–175, Mar. 1968, doi: 10.1109/TAP.1968.1139138.

[13] P. Pal and P. P. Vaidyanathan, "Nested arrays: A novel approach to array processing with enhanced degrees of freedom," *IEEE Trans. Signal Process.*, vol. 58, no. 8, pp. 4167–4181, Aug. 2010, doi: 10.1109/TSP.2010.2049264.

[14] P. P. Vaidyanathan and P. Pal, "Sparse sensing with co-prime samplers and arrays," *IEEE Trans. Signal Process.*, vol. 59, no. 2, pp. 573–586, Feb. 2011, doi: 10.1109/TSP.2010.2089682.

[15] S. Qin, Y. D. Zhang, and M. G. Amin, "Generalized coprime array configurations for direction-of-arrival estimation," *IEEE Trans. Signal Process.*, vol. 63, no. 6, pp. 1377–1390, Mar. 2015, doi: 10.1109/TSP.2015.2393838.

[16] C. L. Liu and P. P. Vaidyanathan, "Super nested arrays: Linear sparse arrays with reduced mutual coupling—Part I: Fundamentals," *IEEE Trans. Signal Peocess.*, vol. 64, no. 15, pp. 3997–4012, Apr. 2016, doi: 10.1109/TSP.2016.2558159.

[17] C. Liu and P. P. Vaidyanathan, "Super nested arrays: Linear sparse arrays with reduced mutual coupling—Part II: High-order extensions," *IEEE Trans. Signal Process.*, vol. 64, no. 16, pp. 4203–4217, Aug. 2016, doi: 10.1109/TSP.2016.2558167.

[18] J. Liu, Y. Zhang, Y. Lu, S. Ren, and S. Cao, "Augmented nested arrays with enhanced DOF and reduced mutual coupling," *IEEE Trans. Signal Process.*, vol. 65, no. 21, pp. 5549–5563, Nov. 2017, doi: 10.1109/TSP.2017.2736493.
[19] P. Pal and P. P. Vaidyanathan, "Coprime sampling and the music algorithm," in *Proc. Digit. Signal Process. Signal Process. Educ. Meeting (DSP/SPE)*, Jan. 2011, pp. 289–294, doi: 10.1109/DSP-SPE.2011.5739227.
[20] R. Cao, B. Liu, F. Gao, and X. Zhang, "A low-complex one-snapshot DOA estimation algorithm with massive ULA," *IEEE Commun. Lett.*, vol. 21, no. 5, pp. 1071–1074, May 2017, doi: 10.1109/LCOMM.2017.2652442.
[21] X. Lai, W. Chen, B. Li, and H. Zeng, "Improved DFT method for DOA estimation with extended coprime array: Based on large difference coarray," *Int. J. Electron.*, vol. 109, no. 5, pp. 733–747, May 2022, doi: 10.1080/00207217.2021.1941289.
[22] S. F. Cotter, "Multiple snapshot matching pursuit for direction of arrival (DOA) estimation," in *Proc. 15th Eur. Signal Process. Conf.*, Sep. 2007, pp. 247–251.
[23] M. Wang and A. Nehorai, "Coarrays, MUSIC, and the Cramér–Rao bound," *IEEE Trans. Signal Process.*, vol. 65, no. 4, pp. 933–946, Feb. 2017, doi: 10.1109/TSP.2016.2626255.
[24] C.-L. Liu and P. P. Vaidyanathan, "Cramér–Rao bounds for coprime and other sparse arrays, which find more sources than sensors," *Digit. Signal Process.*, vol. 61, pp. 43–61, Feb. 2017, doi: 10.1016/j.dsp.2016.04.011.

LIYE ZHANG received the B.S. degree from the National Digital Switching System Engineering and Technological Research Center (NDSC), Zhengzhou, China, in June 2016, where he is currently pursuing the M.S. degree in communications and information systems. His main research interests include array signal processing and wireless communication.

WEIJIA CUI received the M.S. and Ph.D. degrees from the National Digital Switching System Engineering and Technological Research Center (NDSC), Zhengzhou, China, in June 2001 and June 2007, respectively. He is currently working in communications and information system at NDSC. His main research interests include wireless communication theory, satellite and mobile communication, and signal processing.

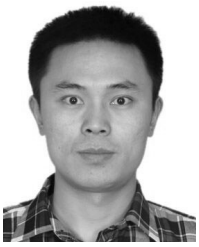

BIN BA received the M.S. and Ph.D. degrees from the National Digital Switching System Engineering and Technological Research Center (NDSC), Zhengzhou, China, in June 2012 and June 2015, respectively. He is currently working in communications and information systems at NDSC. His main research interests include wireless communication theory, signal processing, and parameter estimation.

CHUNXIAO JIAN received the M.S. and Ph.D. degrees from the National University of Defense Technology, Changsha, China, in June 2009 and June 2013, respectively. He is currently working in communications and information system at the National Digital Switching System Engineering and Technological Research Center (NDSC). His main research interests include antenna arrays, satellite communication, and signal processing.

HAO LI received the B.S. degree from the National Digital Switching System Engineering and Technological Research Center (NDSC), Zhengzhou, China, in June 2020, where he is currently pursuing the M.S. degree in communications and information systems. His main research interests include array signal processing and wireless communication.